



Chapter 10

Palau

10.1 Climate Summary

10.1.1 Current Climate

- Warming trends are evident in both annual and half-year mean air temperatures at Koror from 1951. The annual numbers of Warm Days and Warm Nights have increased and the annual number of Cool Days has decreased. These temperature trends are consistent with global warming.
- Annual, half-year and extreme daily rainfall trends show little change at Koror since 1948.
- Tropical cyclones (typhoons) affect Palau mainly between June and November. An average of 28 cyclones per decade developed within or crossed the Palau Exclusive Economic Zone (EEZ) between the 1977 and 2011 seasons. Seventy-three of the 85 tropical cyclones (86%) between the 1981/82 and 2010/11 seasons were weak to moderate events (below Category 3) in the Palau EEZ. Available data are not suitable for assessing long-term trends.

- Variability of wind-waves at Palau is characterised by trade winds and monsoons seasonally, and the El Niño–Southern Oscillation (ENSO) and Inter-Tropical Convergence Zone (ITCZ) location interannually. Available data are not suitable for assessing long-term trends (see Section 1.3).

10.1.2 Climate Projections

For the period to 2100, the latest global climate model (GCM) projections and climate science findings indicate:

- El Niño and La Niña events will continue to occur in the future (*very high confidence*), but there is little consensus on whether these events will change in intensity or frequency;
- Annual mean temperatures and extremely high daily temperatures will continue to rise (*very high confidence*);
- Average rainfall is projected to increase, especially in the wet season (*medium confidence*), along with more extreme rain events (*high confidence*);
- Droughts are projected to decline in frequency (*medium confidence*);
- Ocean acidification is expected to continue (*very high confidence*);
- The risk of coral bleaching will increase in the future (*very high confidence*);
- Sea level will continue to rise (*very high confidence*); and
- A reduction of wave height in December–March is projected in 2090 but not 2035, with a slight decrease in wave period (*low confidence*). In June–September a small decrease in period is projected, with a clockwise rotation toward the south (*low confidence*).

10.2 Data Availability

Palau has five operational meteorological observation stations. Multiple observations within a 24-hour period are taken at Koror and at the Palau International Airport. Climate observations are taken once a day at Kayangel, Nekken and Peleliu. Data are available for Koror from 1924 for rainfall and from 1953 for air temperature. Rainfall data for

the pre World War 2 period have not been used in this report due to uncertainty surrounding the quality of the Japanese era data and the large gap in the record between 1938 and 1948. Koror data from 1948 are homogeneous. Additional information on historical climate trends in the Palau region can be found in the Pacific Climate Change Data Portal www.bom.gov.au/climate/pccsp/.

Wind-wave data from buoys are particularly sparse in the Pacific region, with very short records. Model and reanalysis data are therefore required to detail the wind-wave climate of the region. Reanalysis surface wind data have been used to drive a wave model over the period 1979–2009 to generate a hindcast of the historical wind-wave climate.

10.3 Seasonal Cycles

Information on temperature and rainfall seasonal cycles can be found in Australian Bureau of Meteorology and CSIRO (2011).

10.3.1 Wind-driven Waves

Surface wind-wave driven processes can impact on many aspects of Pacific Island coastal environments, including: coastal flooding during storm wave events; coastal erosion, both during episodic storm events and due to long-term changes in integrated wave climate; characterisation of reef morphology and marine habitat/species distribution; flushing and circulation of lagoons; and potential shipping and renewable wave energy solutions. The surface offshore wind-wave climate can be described by characteristic wave heights, lengths or periods, and directions.

The wind-wave climate of Palau is strongly characterised by the West Pacific Monsoon (WPM) winds and north-easterly trade winds. On the north-west coast near Koror, south-easterly waves are blocked by the island. Waves on the north-west coast are directed from the north-east due to trade winds during December–March with larger wave heights (mean around 3'10" (1.2 m) and longer periods (mean around 7.7 s) than the annual mean (Figure 10.1). Waves are directed from the west and north-east during June–September due to monsoon systems and prevailing trade winds. These waves have smaller heights (mean around 2'3" (0.7 m)) and shorter periods (mean around 6.4 s) than the annual mean (Table 10.1). Waves larger than 8'6" (2.6 m) (99th percentile) occur year round, locally generated in the west by monsoon winds during June–September, and

appearing as long, typically north-westerly swell in December–March due to extra-tropical Northern Hemisphere storms. The height of a 1-in-50 year wave event near Koror is calculated to be 19'9" (6.0 m).

No suitable dataset is available to assess long-term historical trends in the Palau wave climate. However, interannual variability may be assessed in the hindcast record. The wind-wave climate displays strong interannual variability near Koror, varying strongly with the El Niño–Southern Oscillation (ENSO). During La Niña years, wave power is slightly greater than during El Niño years in December–March. Low energy waves are directed from the north-east under La Niña compared to the higher energy waves from the west in June–September under El Niño due to changes in the WPM.

Table 10.1: Mean wave height, period and direction from which the waves are travelling at Palau in December–March and June–September. Observation (hindcast) and climate model simulation mean values are given with the 5–95th percentile range (in brackets). Historical model simulation values are given for comparison with projections (see Section 10.5.6 – Wind-driven waves, and Table 10.7). A compass relating number of degrees to cardinal points (direction) is shown.

		Hindcast Reference Data (1979–2009) north-west Palau	Climate Model Simulations (1986–2005)
Wave Height (metres)	December–March	1.2 (0.7–1.9)	1.8 (1.4–2.2)
	June–September	0.7 (0.2–1.7)	0.8 (0.6–1.2)
Mean Wave Height (feet)	December–March	3.8 (2.2–6.3)	5.8 (4.7–7.1)
	June–September	2.3 (0.6–5.7)	2.7 (2.0–3.8)
Wave Period (seconds)	December–March	7.7 (5.5–10.2)	7.2 (6.6–7.8)
	June–September	6.4 (4.0–9.6)	6.4 (5.7–7.1)
Wave Direction (degrees clockwise from North)	December–March	10 (350–30)	60 (50–70)
	June–September	320 (250–40)	110 (70–200)

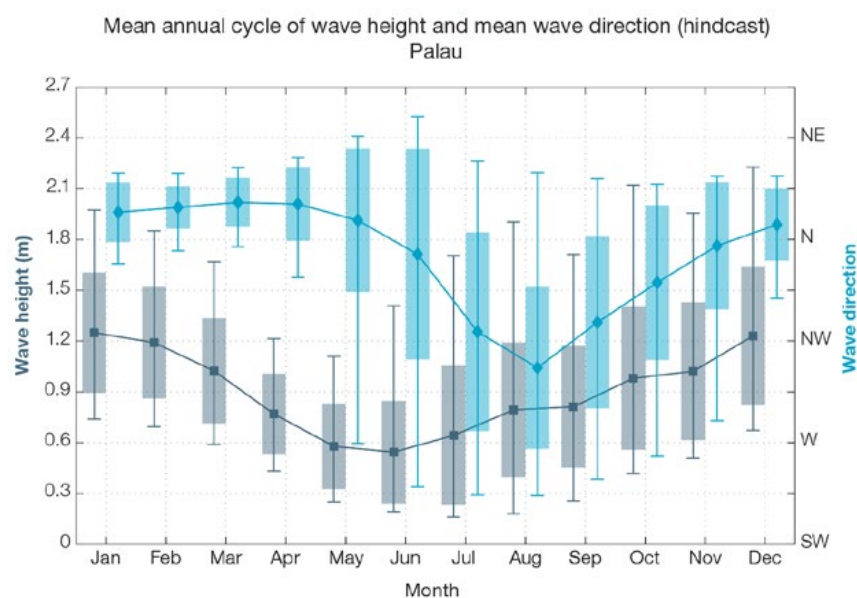


Figure 10.1: Mean annual cycle of wave height (grey) and mean wave direction (blue) at Palau in hindcast data (1979–2009). To give an indication of interannual variability of the monthly means of the hindcast data, shaded boxes show 1 standard deviation around the monthly means, and error bars show the 5–95% range. The direction from which the waves are travelling is shown (not the direction towards which they are travelling).

10.4 Observed Trends

10.4.1 Air Temperature

Annual and Half-year Mean Air Temperature

Mean temperature has increased at Koror since 1951 (Figure 10.2 and Table 10.2). This is largely due to increases in maximum temperature. Only the November–April trend in minimum temperature is statistically significant at the 5% level.

Table 10.2: Annual and half-year trends in air temperature (Tmax, Tmin, Tmean) and rainfall at Koror. The 95% confidence intervals are shown in parentheses. Values for trends significant at the 5% level are shown in boldface.

Koror	Tmax °F/10yrs [°C/10yrs]	Tmin °F/10yrs [°C/10yrs]	Tmean °F/10yrs [°C/10yrs]	Rain inches/10yrs [mm/10yrs]
	1951–2011			
Annual	+0.36 (+0.26, +0.47) [+0.20] (+0.15, +0.26)]	+0.01 (-0.07, +0.08) [+0.01 (-0.04, +0.04)]	+0.18 (+0.13, +0.24) [+0.10] (+0.07, +0.14)]	+0.52 (-2.74, +3.21) [+13.2 (-69.2, +81.5)]
Nov–Apr	+0.33 (+0.23, +0.44) [+0.18] (+0.13, +0.24)]	+0.07 (0.00, +0.13) [+0.04] (0.00, +0.07)]	+0.20 (+0.15, +0.25) [+0.11] (+0.09, +0.14)]	+0.83 (-1.49, +2.92) [+21.1 (-37.9, +74.1)]
May–Oct	+0.36 (+0.27, +0.46) [+0.20] (+0.15, +0.26)]	-0.02 (-0.09, +0.05) [-0.01 (-0.05, +0.03)]	+0.16 (+0.11, +0.23) [+0.09] (+0.06, +0.13)]	-0.13 (-0.49, +0.22) [-3.2 (-12.4, +5.7)]

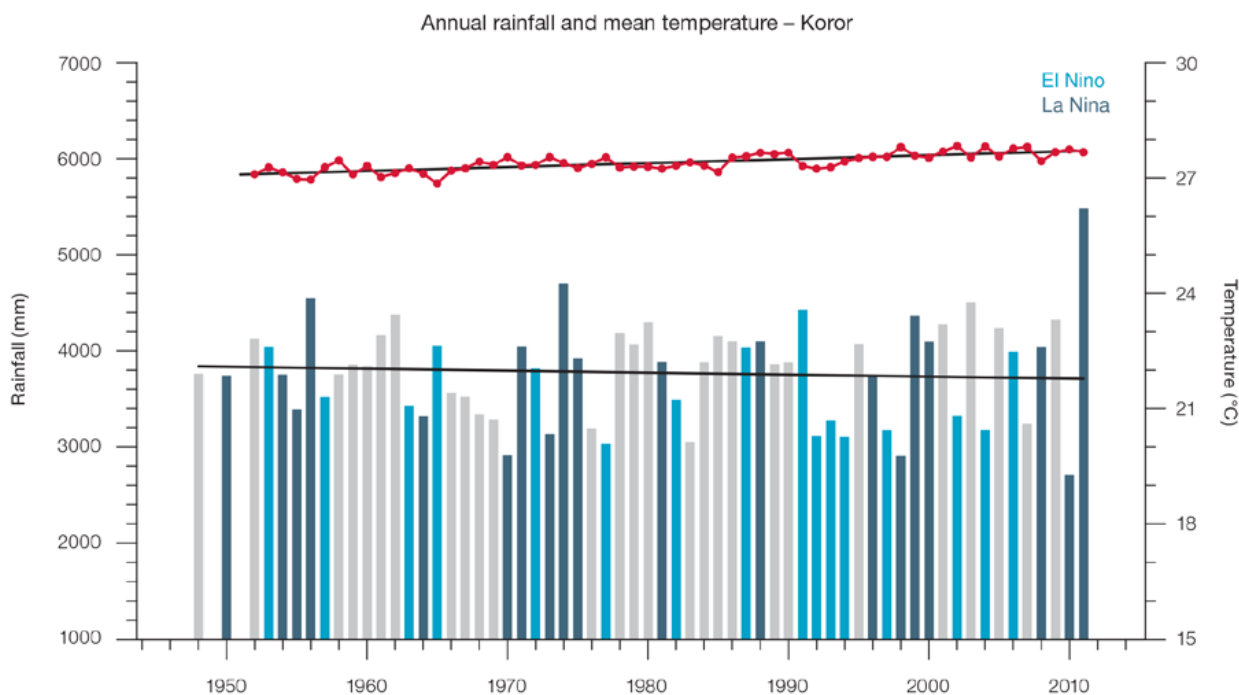


Figure 10.2: Observed time series of annual average values of mean air temperature (red dots and line) and total rainfall (bars) at Koror. Light blue, dark blue and grey bars denote El Niño, La Niña and neutral years respectively. Solid black trend lines indicate a least squares fit.

Extreme Daily Air Temperature

At Koror there have been statistically significant increases in the annual number of Warm Days and Warm Nights and decreases in annual number of Cool Days. Small increases in mean temperatures can have significant impact on temperature extremes, such as the strong trend in Warm Days at Koror. Although this is likely the case, it may also be associated with undiagnosed inhomogeneities in the record. The trend in the annual number of Cool Nights is not significant (Table 10.3 and Figure 10.3).

10.4.2 Rainfall

Annual and Half-year Total Rainfall

Notable interannual variability associated with the ENSO is evident in the observed rainfall record for Koror

since 1948 (Figure 10.2). Trends in annual and half-year rainfall presented in Table 10.2 and Figure 10.2 are not statistically significant at the 5% level. In other words, annual and half-year rainfall trends show little change at Koror.

Daily Rainfall

Daily rainfall trends for Koror are presented in Table 10.3. Due to large year-to-year variability, there are no significant trends in the daily rainfall indices. Figure 10.4 shows insignificant trends in annual Consecutive Dry Days and Max 1-day rainfall.

10.4.3 Tropical Cyclones

When tropical cyclones (typhoons) affect Palau they tend to do so between June and November. The tropical cyclone archive of the Northern Hemisphere indicates that between the

1977 and 2011 seasons, 97 tropical cyclones developed within or crossed the Palau EEZ. This represents an average of 28 cyclones per decade. Refer to Chapter 1, Section 1.4.2 (Tropical Cyclones) for an explanation of the difference in the number of tropical cyclones occurring in Palau in this report (Australian Bureau of Meteorology and CSIRO, 2014) compared to Australian Bureau of Meteorology and CSIRO (2011).

The interannual variability in the number of tropical cyclones in the Palau EEZ is large ranging from zero in some seasons to seven in 1986 (Figure 10.5). The differences between tropical cyclone average occurrence in El Niño, La Niña and neutral years are not statistically significant. Seventy-three of the 85 tropical cyclones (86%) between the 1981/82 and 2010/11 seasons were weak to moderate events (below Category 3) in the Palau EEZ.

Table 10.3: Annual trends in air temperature and rainfall extremes at Koror. The 95% confidence intervals are shown in brackets. Values for trends significant at the 5% level are shown in boldface.

		Koror
TEMPERATURE		1952–2011
Warm Days (days/decade)		+21.03 (+9.03, +37.22)
Warm Nights (days/decade)		+3.53 (+0.80, +5.97)
Cool Days (days/decade)		-6.31 (-9.62, -3.48)
Cool Nights (days/decade)		-0.26 (-4.22, +3.53)
RAINFALL		1948–2011
Rain Days ≥ 1 mm (days/decade)		-0.43 (-4.41, +3.58)
Very Wet Day rainfall	(inches/decade)	-0.04 (-2.46, +2.02)
	(mm/decade)	-1.02 (-62.48, +51.34)
Consecutive Dry Days (days/decade)		+0.36 (-0.16, +0.96)
Max 1-day rainfall	(inches/decade)	-0.07 (-0.37, +0.25)
	(mm/decade)	-1.84 (-9.31, +6.36)

Warm Days: Number of days with maximum temperature greater than the 90th percentile for the base period 1971–2000

Warm Nights: Number of days with minimum temperature greater than the 90th percentile for the base period 1971–2000

Cool Days: Number of days with maximum temperature less than the 10th percentile for the base period 1971–2000

Cool Nights: Number of days with minimum temperature less than the 10th percentile for the base period 1971–2000

Rain Days ≥ 1 mm: Annual count of days where rainfall is greater or equal to 1 mm (0.039 inches)

Very Wet Day rainfall: Amount of rain in a year where daily rainfall is greater than the 95th percentile for the reference period 1971–2000

Consecutive Dry Days: Maximum number of consecutive days in a year with rainfall less than 1 mm (0.039 inches)

Max 1-day rainfall: Annual maximum 1-day rainfall

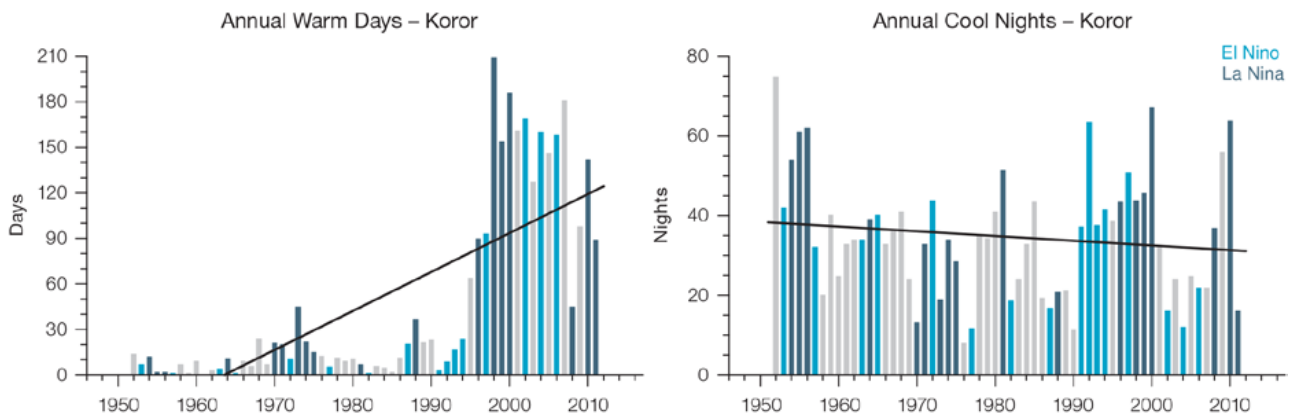


Figure 10.3: Observed time series of annual total number of annual Warm Days (left) and annual Cool Nights (right) at Koror. Solid trend lines indicate a least squares fit.

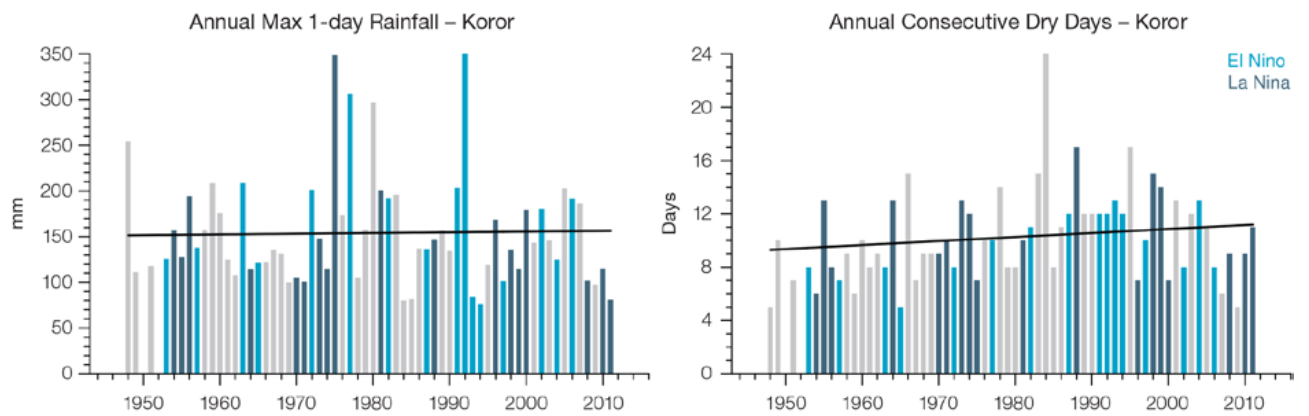


Figure 10.4: Observed time series of annual Consecutive Dry Days (left) and Max 1-day rainfall (right) at Koror. Solid trend lines indicate a least squares fit.

Long term trends in frequency and intensity have not been presented as country scale assessment is not recommended. Some tropical cyclone tracks analysed in this subsection include the tropical depression stage (sustained winds less than or equal to 34 knots) before and/or after tropical cyclone formation.

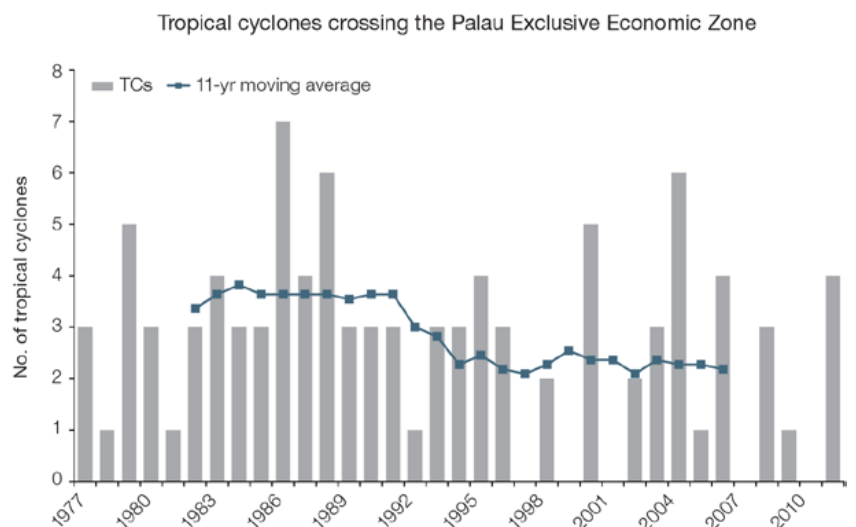


Figure 10.5: Time series of the observed number of tropical cyclones developing within and crossing the Palau EEZ per season. The 11-year moving average is in blue.

10.5 Climate Projections

The performance of the available Coupled Model Intercomparison Project (Phase 5) (CMIP5) climate models over the Pacific has been rigorously assessed (Brown et al., 2013a, b; Grose et al., 2014; Widlansky et al., 2013). The simulation of the key processes and features for the Palau region is similar to the previous generation of CMIP3 models, with all the same strengths and many of the same weaknesses. The best-performing CMIP5 models used here have lower biases (differences between the simulated and observed climate data) than the best CMIP3 models, and there are fewer poorly-performing models. For Palau, the most important model bias is that the westerly winds of the monsoon do not extend far enough east in many models, and the position of the monsoon region and the Inter-Tropical Convergence Zone (ITCZ) are not correct, producing overly

wet conditions in November–April and dry conditions in May–October. This affects the confidence in the model projections. Out of 27 models assessed, one model was rejected for use in these projections due to biases in the mean climate. Climate projections have been derived from up to 26 new GCMs in the CMIP5 database (the exact number is different for each scenario, Appendix A), compared with up to 18 models in the CMIP3 database reported in Australian Bureau of Meteorology and CSIRO (2011).

It is important to realise that the models used give different projections under the same scenario. This means there is not a single projected future for Palau, but rather a range of possible futures for each emission scenario. This range is described below.

10.5.1 Temperature

Further warming is expected over Palau (Figure 10.6, Table 10.6). Under all RCPs, the warming is up to 1.0°C by 2030, relative to 1995, but after 2030 there is a growing difference in warming between each RCP. For example, in Palau by 2090 a warming of 2.1 to 4.0°C is projected for RCP8.5 while a warming of 0.4–1.2°C is projected for RCP2.6. This range is broader than that presented in Australian Bureau of Meteorology and CSIRO (2011) because a wider range of emissions scenarios is considered. While relatively warm and cool years and decades will still occur due to natural variability, there is projected to be more warm years and decades on average in a warmer climate.

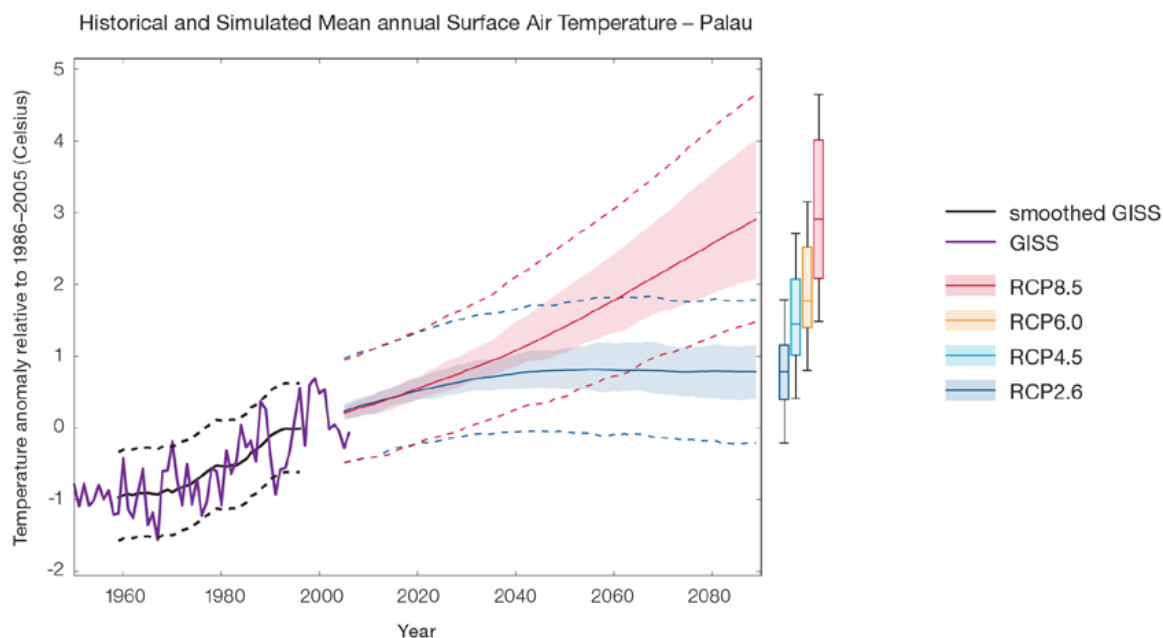


Figure 10.6: Historical and simulated surface air temperature time series for the region surrounding Palau. The graph shows the anomaly (from the base period 1986–2005) in surface air temperature from observations (the GISS dataset, in purple), and for the CMIP5 models under the very high (RCP8.5, in red) and very low (RCP2.6, in blue) emissions scenarios. The solid red and blue lines show the smoothed (20-year running average) multi-model mean anomaly in surface air temperature, while shading represents the spread of model values (5–95th percentile). The dashed lines show the 5–95th percentile of the observed interannual variability for the observed period (in black) and added to the projections as a visual guide (in red and blue). This indicates that future surface air temperature could be above or below the projected long-term averages due to interannual variability. The ranges of projections for a 20-year period centred on 2090 are shown by the bars on the right for RCP8.5, 6.0, 4.5 and 2.6.

There is *very high confidence* that temperatures will rise because:

- It is known from theory and observations that an increase in greenhouse gases will lead to a warming of the atmosphere; and
- Climate models agree that the long-term average temperature will rise.

There is *medium confidence* in the model average temperature change shown in Table 10.6 because:

- The new models do not match temperature changes in the recent past in the Palau as well as in other places, possibly due to problems with the observed records or with the models; and
- There is a bias in the simulation of the ITCZ, affecting the uncertainty the projections of rainfall but also temperature.

10.5.2 Rainfall

The long-term average rainfall is projected by almost all models to increase. The increase is greater for the higher emissions scenarios, especially towards the end of the century (Figure 10.7, Table 10.6). Similar to the CMIP3 results, more than 80% of models project an increase in May–October rainfall. The models show little change for November–April rainfall. The year-to-year rainfall variability over Palau is much larger than the projected change, even in the upper range of models in the highest emission scenario by 2090. There will still be wet and dry years and decades due to natural variability, but most models show that the long-term average is

expected to be wetter. The effect of climate change on average rainfall may not be obvious in the short or medium term due to natural variability. These results are similar to those reported in Australian Bureau of Meteorology and CSIRO (2011).

There is general agreement between models that rainfall will increase. However there is a significant bias in the position of the WPM in the models and this lowers the confidence in the magnitude of the projected changes. The 5–95th percentile range of projected values from CMIP5 climate models is large, e.g. for example in Palau North in RCP8.5 the range is -5 to +8% by 2030 and -4–25% by 2090.

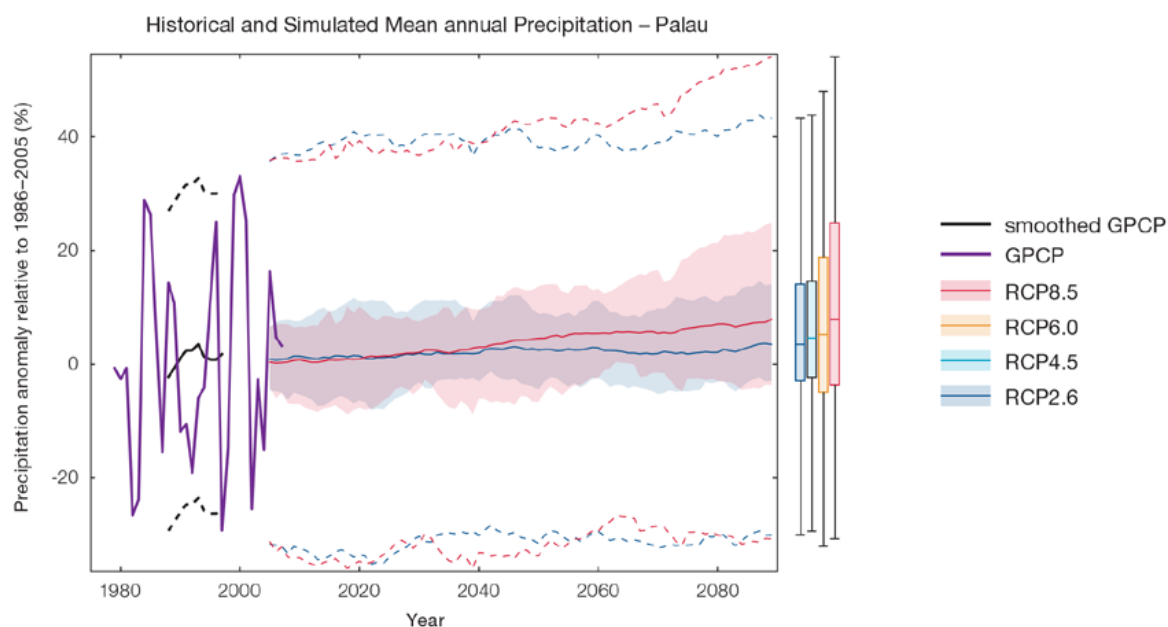


Figure 10.7: Historical and simulated annual average rainfall time series for the region surrounding Palau. The graph shows the anomaly (from the base period 1986–2005) in rainfall from observations (the GPCP dataset, in purple), and for the CMIP5 models under the very high (RCP8.5, in red) and very low (RCP2.6, in blue) emissions scenarios. The solid red and blue lines show the smoothed (20-year running average) multi-model mean anomaly in rainfall, while shading represents the spread of model values (5–95th percentile). The dashed lines show the 5–95th percentile of the observed interannual variability for the observed period (in black) and added to the projections as a visual guide (in red and blue). This indicates that future rainfall could be above or below the projected long-term averages due to interannual variability. The ranges of projections for a 20-year period centred on 2090 are shown by the bars on the right for RCP8.5, 6.0, 4.5 and 2.6.

There is *medium confidence* that the long-term rainfall over Palau will increase because:

- The majority of CMIP3 and CMIP5 models agree that the rainfall in the WPM and ITCZ will increase under a warmer climate; and
- There are well-understood physical reasons why a warmer climate will lead to increased rainfall in the ITCZ region.

There is *medium confidence* in the model average rainfall change shown in Table 10.6 because:

- The complex set of processes involved in tropical rainfall is challenging to simulate in models. This means that the confidence in the projection of rainfall is generally lower than for other variables such as temperature;
- The new CMIP5 models broadly simulate the influence from the key features such as the WPM and the ITCZ, but have some uncertainty and biases, similar to the old CMIP3 models; and
- The future behaviour of the ENSO is unclear, and the ENSO strongly influences year-to-year rainfall variability.

10.5.3 Extremes

Extreme Temperature

The temperature on extremely hot days is projected to increase by about the same amount as average temperature. This conclusion is based on analysis of daily temperature data from a subset of CMIP5 models (Chapter 1). The frequency of extremely hot days is also expected to increase.

The temperature of the 1-in-20-year hot day is projected to increase by approximately 0.7°C by 2030 under the RCP2.6 scenario and by 0.8°C under the RCP8.5 scenario. By 2090 the projected increase is 0.8°C for RCP2.6 and 3.2°C for RCP8.5.

There is *very high confidence* that the temperature of extremely hot days and the temperature of extremely cool days will increase, because:

- A change in the range of temperatures, including the extremes, is physically consistent with rising greenhouse gas concentrations;
- This is consistent with observed changes in extreme temperatures around the world over recent decades (IPCC, 2012); and
- All the CMIP5 models agree on an increase in the frequency and intensity of extremely hot days and a decrease in the frequency and intensity of cool days.

There is *low confidence* in the magnitude of projected change in extreme temperature because models generally underestimate the current intensity and frequency of extreme events. Changes to the particular driver of extreme temperatures affect whether the change to extremes is more or less than the change in the average temperature, and the changes to the drivers of extreme temperatures in Palau are currently unclear. Also, while all models project the same direction of change there is a wide range in the projected magnitude of change among the models.

Extreme Rainfall

The frequency and intensity of extreme rainfall events are projected to increase. This conclusion is based on analysis of daily rainfall data from a subset of CMIP5 models using a similar method to that in Australian Bureau of Meteorology and CSIRO (2011) with some improvements (Chapter 1), so the results are slightly different to those in Australian Bureau of Meteorology and CSIRO (2011). The current 1-in-20-year daily rainfall amount is projected to increase by approximately 18 mm by 2030 for RCP2.6 and by 13 mm by 2030 for RCP8.5. By 2090, it is projected to increase by approximately 19 mm for RCP2.6 and by 50 mm for RCP8.5. The majority of models project the current 1-in-20-year daily rainfall event will become, on average, a 1-in-8-year event for RCP2.6 and a 1-in-4-year event for RCP8.5 by 2090. These results are different to those found in Australian Bureau of Meteorology and CSIRO (2011) because of different methods used (Chapter 1).

There is *high confidence* that the frequency and intensity of extreme rainfall events will increase because:

- A warmer atmosphere can hold more moisture, so there is greater potential for extreme rainfall (IPCC, 2012); and
- Increases in extreme rainfall in the Pacific are projected in all available climate models.

There is *low confidence* in the magnitude of projected change in extreme rainfall because:

- Models generally underestimate the current intensity of local extreme events, especially in this area due to the ‘cold-tongue bias’ (Chapter 1);
- Changes in extreme rainfall projected by models may be underestimated because models seem to underestimate the observed increase in heavy rainfall with warming (Min et al., 2011);
- GCMs have a coarse spatial resolution, so they do not adequately capture some of the processes involved in extreme rainfall events; and
- The Conformal Cubic Atmospheric Model (CCAM) downscaling model has finer spatial resolution and the CCAM results presented in Australian Bureau of Meteorology and CSIRO (2011) indicates a smaller increase in the number of extreme rainfall days, and there is no clear reason to accept one set of models over another.

Drought

Drought projections (defined in Chapter 1) are described in terms of changes in proportion of time in drought, frequency and duration by 2090 for very low and very high emissions (RCP 2.6 and 8.5).

For Palau the overall proportion of time spent in drought is expected to decrease under all scenarios. Under RCP8.5 the frequency of drought in all categories is projected to decrease (Figure 10.8). The duration of moderate, severe and extreme drought events is projected to decrease while the duration of mild drought events is projected to remain stable under RCP8.5. Under RCP2.6 the frequency of mild and moderate drought is projected to decrease while the frequency of severe and extreme drought is projected to remain stable. The duration of events in all categories is projected to remain stable under RCP2.6. These results are similar to those reported in Australian Bureau of Meteorology and CSIRO (2011).

There is *medium confidence* in this direction of change because:

- There is only *medium confidence* in the direction of mean rainfall change;
- These drought projections are based upon a subset of models; and
- Like the CMIP3 models, the majority of the CMIP5 models agree on this direction of change.

There is *medium confidence* in the projections of drought frequency and duration because there is *medium confidence* in the magnitude of rainfall projections, and no consensus about projected changes in the ENSO, which directly influence the projection of drought.

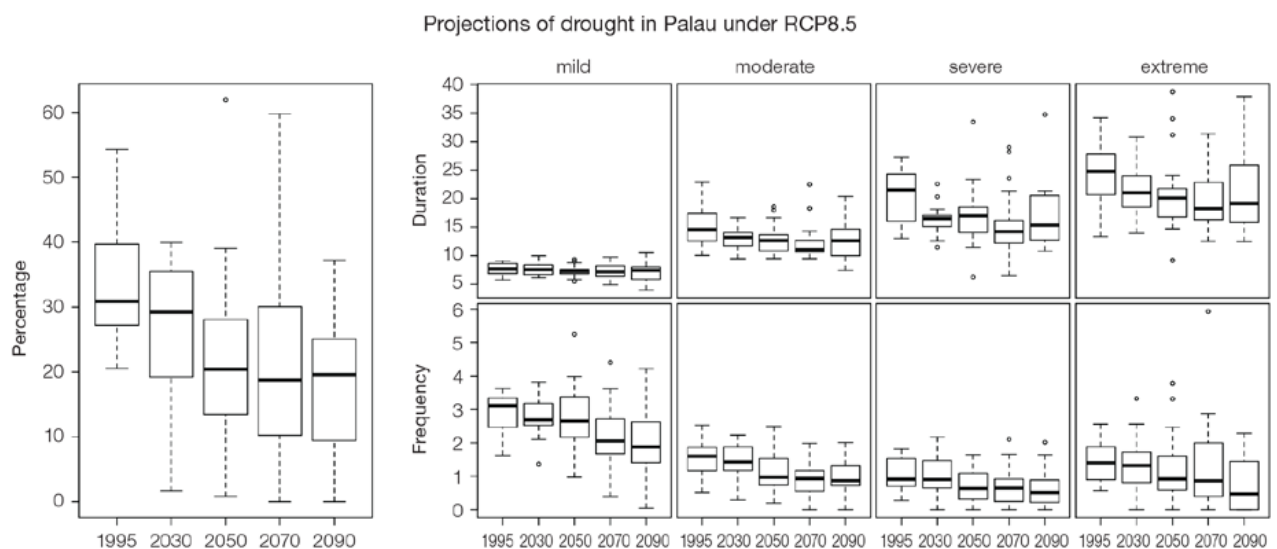


Figure 10.8: Box-plots showing percent of time in moderate, severe or extreme drought (left hand side), and average drought duration and frequency for the different categories of drought (mild, moderate, severe and extreme) for Palau. These are shown for 20-year periods centred on 1995, 2030, 2050, 2070 and 2090 for the RCP8.5 (very high emissions) scenario. The thick dark lines show the median of all models, the box shows the interquartile (25–75%) range, the dashed lines show 1.5 times the interquartile range and circles show outlier results.

Tropical Cyclones

Global Picture

There is a growing level of agreement among models that on a global basis the frequency of tropical cyclones is likely to decrease by the end of the 21st century. The magnitude of the decrease varies from 6–35% depending on the modelling study. There is also a general agreement between models that there will be an increase in the mean maximum wind speed of cyclones by between 2% and 11% globally, and an increase in rainfall rates of the order of 20% within 100 km of the cyclone centre (Knutson et al., 2010). Thus, the scientific community has a *medium* level of confidence in these global projections.

Palau

The projection is for a decrease in tropical cyclone genesis (formation) frequency for the northern basin (see Figure 10.9 and Table 10.4). However the confidence level for this projection is low.

The GCMs show inconsistent results across models for changes in tropical cyclone frequency for the northern basin, using either the direct detection methodologies (CVP or CDD) or the empirical methods described in Chapter 1. The direct detection methodologies tend to indicate a decrease in formation with almost half of results suggesting decreases of between 20–50%. The empirical techniques assess changes in the main atmospheric ingredients known to be necessary for tropical cyclone formation. About four-fifths of results suggest the conditions for tropical cyclone formation will become more favourable in this region. However, when only the models for which direct detection and empirical methods are available are considered, the assessment is for a decrease in tropical cyclone formation. These projections are consistent with those of Australian Bureau of Meteorology and CSIRO (2011).

Table 10.4: Projected percentage change in cyclone frequency in the northern basin (0–15°N; 130–180°E) for 22 CMIP5 climate models, based on five methods, for 2080–2099 relative to 1980–1999 for RCP8.5 (very high emissions). 22 CMIP5 climate models were selected based upon the availability of data or on their ability to reproduce a current-climate tropical cyclone climatology (See Section 1.5.3 – Detailed Projection Methods, Tropical Cyclones). Blue numbers indicate projected decreases in tropical cyclone frequency, red numbers an increase. MMM is the multi-model mean change. N increase is the proportion of models (for the individual projection method) projecting an increase in cyclone formation.

Model	GPI change	GPI-M change	Tippett	CDD	OWZ
access10	71	22	-54	71	
access13	55	48	-33	107	
bccrsm11	13	11	-22		2
canesm2	34	22	-47	24	
ccsm4				-81	-12
cnrm_cm5	0	-2	-25	-1	-23
csiro_mk36	7	-1	-30	8	15
fgoals_g2	-5	-15	-10		
fgoals_s2	-3	-3	-35		
gfdl-esm2m				-2	-8
gfdl_cm3	15	5	-17		-40
gfdl-esm2g				-33	-37
gisse2r	14	9	-17		
hadgem2_es	13	1	-57		
inm	25	26	-5		
ipslcm5alr	19	9	-17		
ipslcm5blr				-49	
miroc5				-52	-50
miroc5m	17	2	26		
mpim	19	17	-45		
mrikgcm3	1	-3	-34		
noresm1m	-11	-17	-19	-42	
MMM	17	8	-26	-5	-19
N increase	0.8	0.7	0.1	0.4	0.3

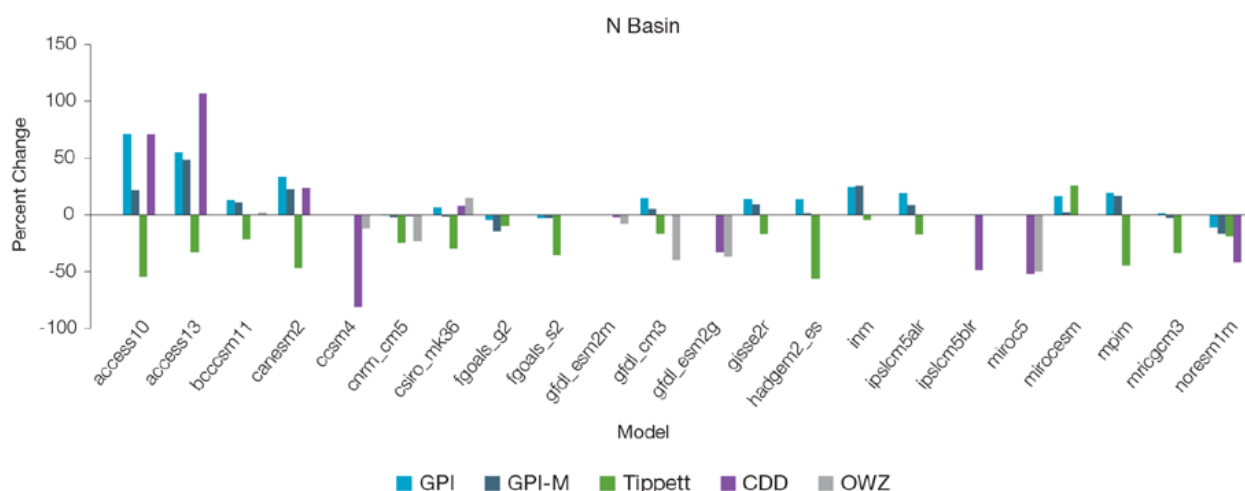


Figure 10.9: Projected percentage change in cyclone frequency in the northern basin (data from Table 10.4).

10.5.4 Coral Reefs and Ocean Acidification

As atmospheric CO₂ concentrations continue to rise, oceans will warm and continue to acidify. These changes will impact the health and viability of marine ecosystems, including coral reefs that provide many key ecosystem services (*high confidence*). These impacts are also likely to be compounded by other stressors such as storm damage, fishing pressure and other human impacts.

The projections for future ocean acidification and coral bleaching use three RCPs (2.6, 4.5, and 8.5).

Ocean Acidification

Ocean acidification is expressed in terms of aragonite saturation state (Chapter 1). In Palau the aragonite saturation state has declined from about 4.5 in the late 18th century to an observed value of about 3.9 ± 0.1 by 2000 (Kuchinke et al., 2014). All models show that the aragonite saturation state, a proxy for coral reef growth rate, will continue to decrease as atmospheric CO₂ concentrations increase (*very high confidence*). Projections from CMIP5 models indicate that under RCPs 8.5 and 4.5 the median aragonite saturation state will transition to marginal conditions (3.5) around 2030. In RCP8.5 the aragonite saturation state continues to strongly decline thereafter to values where coral reefs have not historically

been found (< 3.0). Under RCP4.5 the aragonite saturation plateaus around 3.2 i.e. marginal conditions for healthy coral reefs. While under RCP2.6 the median aragonite saturation state never falls below 3.5, and increases slightly toward the end of the century (Figure 10.10) suggesting that the conditions remains adequate for healthy corals reefs. There is *medium confidence* in this range and distribution of possible futures because the projections are based on climate models that do not resolve the reef scale that can play a role in modulating large-scale changes. The impacts of ocean acidification are also likely to affect the entire marine ecosystem impacting the key ecosystem services provided by reefs.

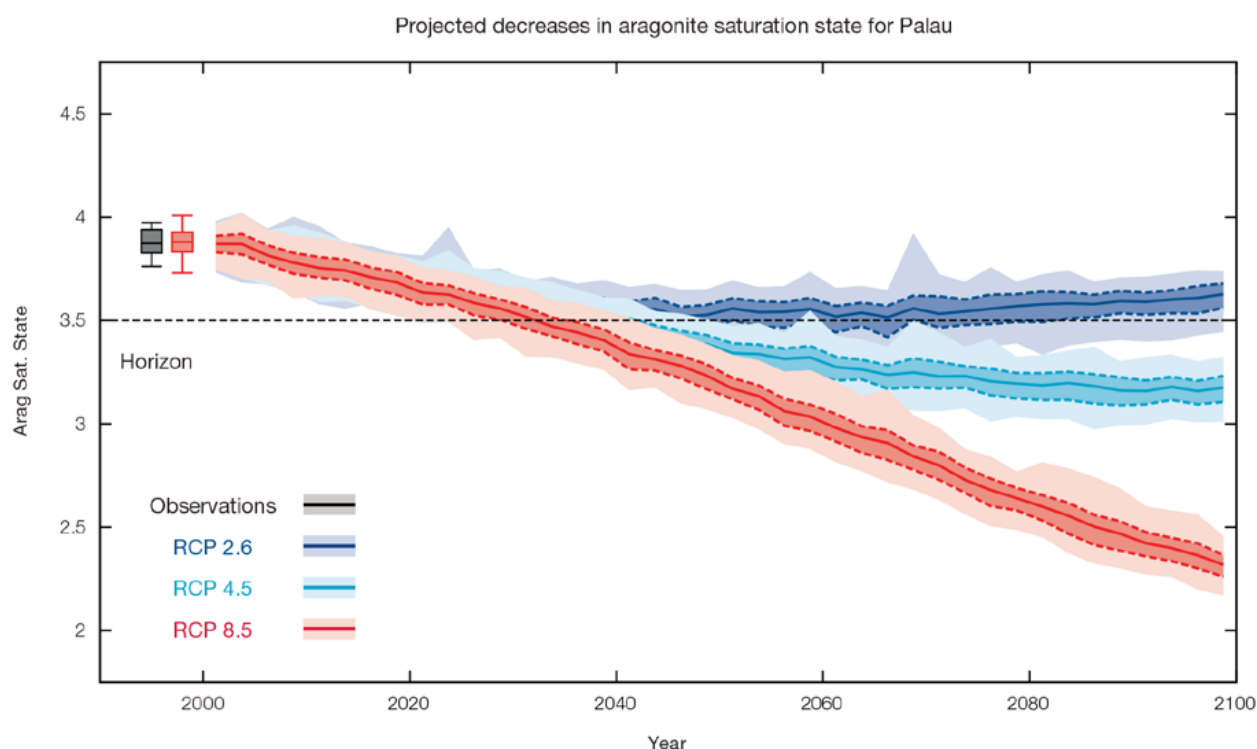


Figure 10.10: Projected decreases in aragonite saturation state in Palau from CMIP5 models under RCP2.6, 4.5 and 8.5. Shown are the median values (solid lines), the interquartile range (dashed lines), and 5% and 95% percentiles (light shading). The horizontal line represents the transition to marginal conditions for coral reef health (from Guinotte et al., 2003).

Coral Bleaching Risk

As the ocean warms, the risk of coral bleaching increases (*very high confidence*). There is *medium confidence* in the projected rate of change for Palau because there is *medium confidence* in the rate of change of sea-surface temperature (SST), and the changes at the reef scale (which can play a role in modulating large-scale changes) are not adequately resolved. Importantly, the coral bleaching risk calculation does not account the impact of other potential stressors (Chapter 1).

The changes in the frequency (or recurrence) and duration of severe bleaching risk are quantified for different projected SST changes (Table 10.5). Overall there is a

decrease in the time between two periods of elevated risk and an increase in the duration of the elevated risk. For example, under a long-term mean increase of 1°C (relative to 1982–1999 period), the average period of severe bleaching risk (referred to as a risk event will last 8.9 weeks (with a minimum duration of 1.7 weeks and a maximum duration of 6.4 months) and the average time between two risks will be 2.0 years (with the minimum recurrence of 1.9 months and a maximum recurrence of 8.2 years). If severe bleaching events occur more often than once every five years, the long-term viability of coral reef ecosystems becomes threatened.

10.5.5 Sea Level

Mean sea level is projected to continue to rise over the course of the 21st century. There is *very high confidence* in the direction of change. The CMIP5 models simulate a rise of between approximately 8–18 cm by 2030 (*very similar values for different RCPs*), with increases of 41–88 cm by 2090 under the RCP8.5 (Figure 10.11 and Table 10.6). There is *medium confidence* in the range mainly because there is still uncertainty associated with projections of the Antarctic ice sheet contribution. Interannual variability of sea level will lead to periods of lower and higher regional sea levels. In the past, this interannual variability has been about 36 cm (5–95% range, after removal of the seasonal signal, see dashed lines in Figure 10.11 (a) and it is likely that a similar range will continue through the 21st century.

Table 10.5: The impacts of increasing SST on severe coral bleaching risk for the Palau EEZ.

Temperature change ¹	Recurrence interval ²	Duration of the risk event ³
Change in observed mean	30 years	4.9 weeks
+0.25°C	29.1 years (28.4 years – 29.8 years)	9.3 weeks (4.9 weeks – 5.7 weeks)
+0.5°C	28.8 years (28.4 years – 29.1 years)	3.7 months (3.6 months – 3.8 months)
+0.75°C	7.3 years (2.6 years – 13.6 years)	7.4 weeks (3.1 weeks – 5.1 months)
+1°C	2.0 years (1.9 months – 8.2 years)	8.9 weeks (1.7 weeks – 6.4 months)
+1.5°C	4.5 months (0.8 months – 1.1 years)	3.0 months (1.8 weeks – 9.8 months)
+2°C	2.7 months (0.8 months – 4.7 months)	8.8 months (9.7 months – 2.7 years)

¹ This refers to projected SST anomalies above the mean for 1982–1999.

² Recurrence is the mean time between severe coral bleaching risk events. Range (min – max) shown in brackets.

³ Duration refers to the period of time where coral are exposed to the risk of severe bleaching. Range (min – max) shown in brackets.

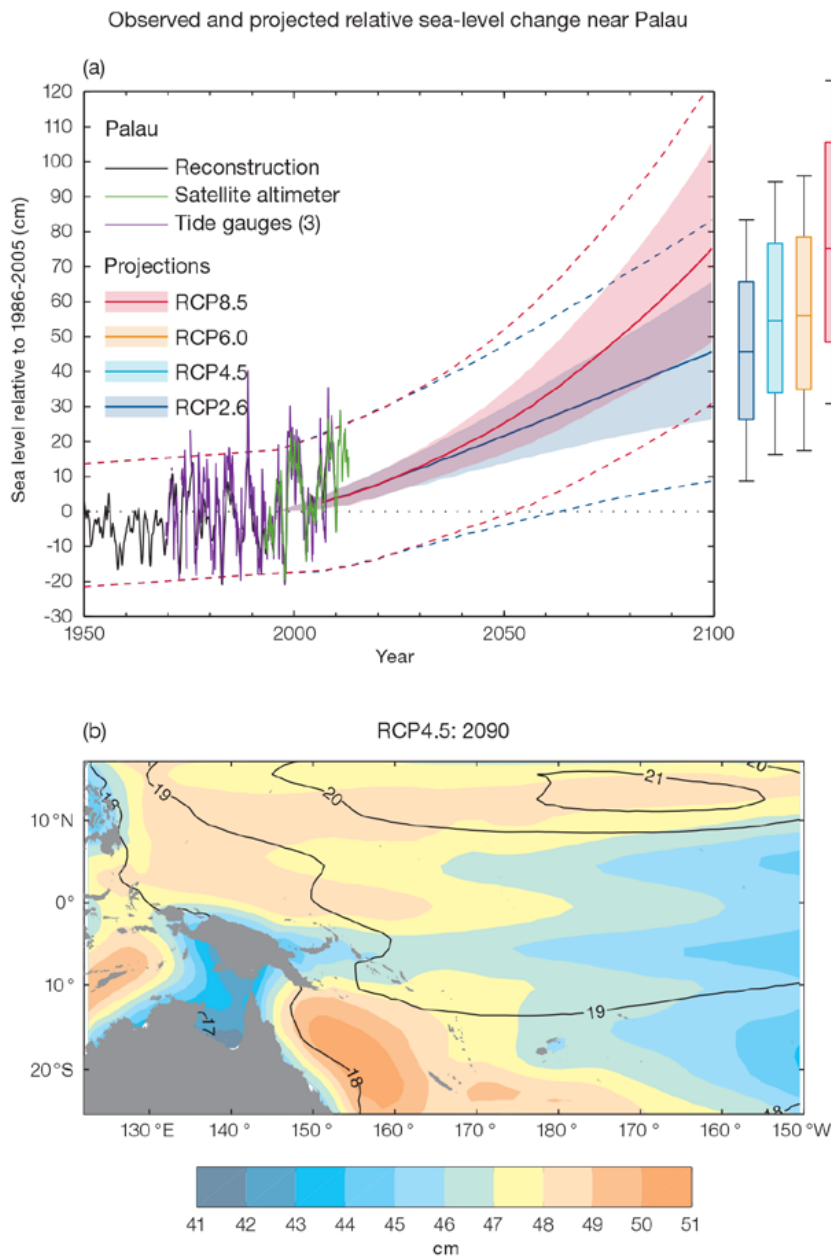


Figure 10.11: (a) The observed tide-gauge records of relative sea-level (since the late 1970s) are indicated in purple, and the satellite record (since 1993) in green. The gridded (reconstructed) sea level data at Palau (since 1950) is shown in black. Multi-model mean projections from 1995–2100 are given for the RCP8.5 (red solid line) and RCP2.6 emissions scenarios (blue solid line), with the 5–95% uncertainty range shown by the red and blue shaded regions. The ranges of projections for four emission scenarios (RCPs 2.6, 4.5, 6.0 and 8.5) by 2100 are also shown by the bars on the right. The dashed lines are an estimate of interannual variability in sea level (5–95% uncertainty range about the projections) and indicate that individual monthly averages of sea level can be above or below longer-term averages.

(b) The regional distribution of projected sea level rise under the RCP4.5 emissions scenario for 2081–2100 relative to 1986–2005. Mean projected changes are indicated by the shading, and the estimated uncertainty in the projections is indicated by the contours (in cm).

10.5.6 Wind-driven Waves

During December–March in Palau, there is a projected decrease in wave heights in 2090 (Figure 10.12) which is significant in January and February under RCP8.5, but no change is projected in 2035 (*low confidence*) (Table 10.7). Wave period is projected to decrease slightly, particularly in February and March (significant in March under RCP4.5 and RCP8.5, in 2090 and in 2035 under RCP8.5) (*low confidence*). No significant change is projected in wave direction (*low confidence*). These changes are characteristic of a decrease in the prevailing north-easterly trade winds.

There is a suggested small decrease in the height of the larger waves in 2090 under RCP8.5 (*low confidence*).

In June–September (the monsoon season), there is no change in projected in wave height, but a small decrease is projected in wave period, significant in September in 2090 under both emissions scenarios (*low confidence*) (Table 10.7). A clockwise rotation (toward the south) is suggested in 2090 and in 2035 under RCP4.5, significant in September by 2090 under RCP8.5, and direction is projected to be more variable than in the dry season, similar to the present climate (*low confidence*).

There is *low confidence* in projected changes in the Palau wind-wave climate because:

- Projected changes in wave climate are dependent on confidence in projected changes in the ENSO, which is low; and
- The differences between simulated and observed (hindcast) wave data are larger than the projected wave changes, which further reduces our confidence in projections.

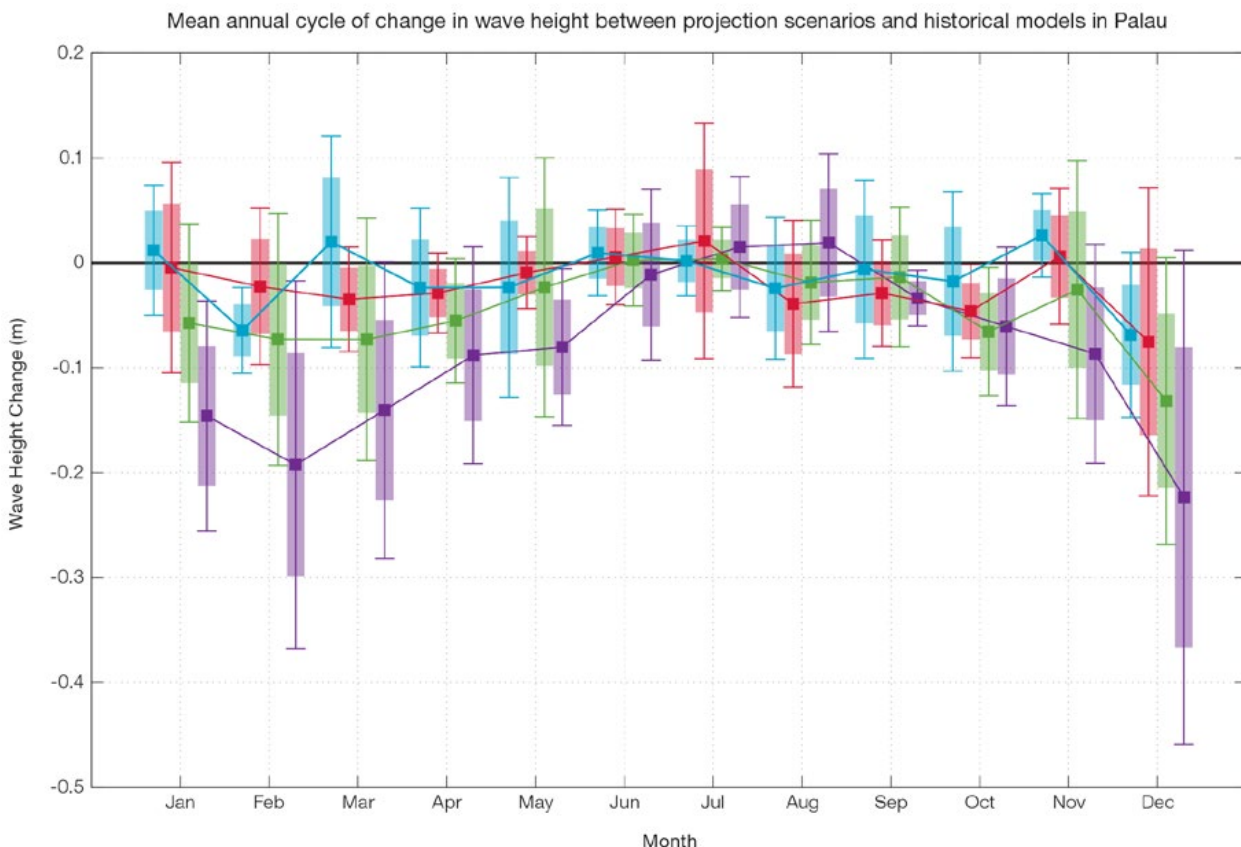


Figure 10.12: Mean annual cycle of change in wave height between projection scenarios and historical models in Palau. This panel shows a projected decrease in wave height in December–March in 2090, with no change in June–September. Shaded boxes show 1 standard deviation of models' means around the ensemble means, and error bars show the 5–95% range inferred from the standard deviation. Colours represent RCP scenarios and time periods: blue 2035 RCP4.5 (low emissions), red 2035 RCP8.5 (very high emissions), green 2090 RCP4.5 (low emissions), purple 2090 RCP8.5 (very high emissions).

10.5.7 Projections Summary

There is *very high confidence* in the direction of long-term change in a number of key climate variables, namely an increase in mean and extremely high temperatures, sea level and ocean acidification. There is *high confidence* that the frequency and intensity of extreme rainfall will increase. There is *high confidence* that mean annual rainfall will increase, and

medium confidence in a decrease in drought frequency.

Tables 10.6 and 10.7 quantify the mean changes and ranges of uncertainty for a number of variables, years and emissions scenarios. A number of factors are considered in assessing confidence, i.e. the type, amount, quality and consistency of evidence (e.g. mechanistic understanding, theory, data, models, expert judgment) and the degree

of agreement, following the IPCC guidelines (Mastrandrea et al., 2010). Confidence ratings in the projected magnitude of mean change are generally lower than those for the direction of change (see paragraph above) because magnitude of change is more difficult to assess. For example, there is *very high confidence* that temperature will increase, but *medium confidence* in the magnitude of mean change.

Table 10.6: Projected changes in the annual and seasonal mean climate for Palau under four emissions scenarios; RCP2.6 (very low emissions, in dark blue), RCP4.5 (low emissions, in light blue), RCP6 (medium emissions, in orange) and RCP8.5 (very high emissions, in red). Projected changes are given for four 20-year periods centred on 2030, 2050, 2070 and 2090, relative to a 20-year period centred on 1995. Values represent the multi-model mean change, with the 5–95% range of uncertainty in brackets. Confidence in the magnitude of change is expressed as *high*, *medium* or *low*. Surface air temperatures in the Pacific are closely related to sea-surface temperatures (SST), so the projected changes to air temperature given in this table can be used as a guide to the expected changes to SST. (See also Section 1.5.2). 'NA' indicates where data are not available.

Variable	Season	2030	2050	2070	2090	Confidence (magnitude of change)
Surface air temperature (°C)	Annual	0.6 (0.5–0.9)	0.8 (0.6–1.1)	0.8 (0.5–1.2)	0.8 (0.4–1.2)	<i>Medium</i>
		0.7 (0.5–1)	1 (0.7–1.4)	1.3 (0.9–1.8)	1.4 (1–2.1)	
		0.6 (0.4–0.9)	0.9 (0.7–1.4)	1.4 (1.1–1.9)	1.8 (1.4–2.5)	
		0.8 (0.6–1)	1.4 (1–1.9)	2.2 (1.6–3.1)	3 (2.1–4)	
Maximum temperature (°C)	1-in-20 year event	0.7 (0.2–1)	0.8 (0.3–1.1)	0.8 (0.2–1.1)	0.8 (0.1–1.1)	<i>Medium</i>
		0.7 (0.4–1.1)	1 (0.5–1.4)	1.3 (0.7–1.6)	1.4 (0.9–2)	
		NA (NA–NA)	NA (NA–NA)	NA (NA–NA)	NA (NA–NA)	
		0.8 (0.4–1.2)	1.5 (0.9–2.2)	2.3 (1.6–3.3)	3.2 (2–4.4)	
Minimum temperature (°C)	1-in-20 year event	0.7 (0.4–1.1)	0.7 (0.3–1)	0.7 (0.2–0.9)	0.7 (0.3–1)	<i>Medium</i>
		0.6 (0.4–0.8)	0.9 (0.6–1.2)	1.2 (0.6–1.6)	1.3 (0.9–1.7)	
		NA (NA–NA)	NA (NA–NA)	NA (NA–NA)	NA (NA–NA)	
		0.8 (0.4–1)	1.5 (1.1–2)	2.3 (1.5–3.2)	3.2 (2.3–4.1)	
Total rainfall (%)	Annual	2 (-4–10)	3 (-4–10)	2 (-5–9)	3 (-3–14)	<i>Medium</i>
		3 (-8–9)	3 (-5–11)	5 (-6–14)	5 (-2–15)	
		1 (-7–8)	3 (-4–11)	3 (-6–14)	5 (-5–19)	
		2 (-5–8)	4 (-7–13)	6 (-2–16)	8 (-4–25)	
Total rainfall (%)	Nov-Apr	1 (-7–12)	1 (-8–11)	0 (-10–8)	3 (-7–13)	<i>Low</i>
		2 (-6–10)	1 (-13–12)	4 (-12–16)	3 (-10–10)	
		1 (-7–11)	2 (-7–10)	2 (-10–17)	3 (-10–20)	
		1 (-5–10)	3 (-11–14)	2 (-12–14)	3 (-15–19)	
Total rainfall (%)	May-Oct	3 (-2–9)	6 (-1–13)	5 (-1–12)	5 (-1–14)	<i>Medium</i>
		4 (-5–15)	5 (-2–11)	8 (-2–19)	8 (-1–17)	
		1 (-6–6)	4 (-2–18)	5 (-2–13)	8 (0–20)	
		3 (-3–9)	7 (-1–15)	10 (3–20)	14 (1–38)	
Aragonite saturation state (Ωar)	Annual	-0.3 (-0.6–0.1)	-0.4 (-0.7–0.1)	-0.4 (-0.6–0.2)	-0.3 (-0.6–0.1)	<i>Medium</i>
		-0.3 (-0.6–0.1)	-0.6 (-0.8–0.3)	-0.7 (-0.9–0.5)	-0.8 (-1.0–0.5)	
		NA (NA–NA)	NA (NA–NA)	NA (NA–NA)	NA (NA–NA)	
		-0.4 (-0.6–0.2)	-0.7 (-1.0–0.5)	-1.1 (-1.4–0.9)	-1.5 (-1.7–1.2)	
Mean sea level (cm)	Annual	13 (8–17)	22 (14–30)	32 (20–44)	42 (25–59)	<i>Medium</i>
		12 (8–17)	23 (15–31)	35 (23–48)	48 (30–67)	
		12 (8–17)	22 (14–30)	34 (22–47)	49 (31–68)	
		13 (8–18)	26 (17–35)	43 (28–58)	64 (41–88)	

Waves Projections Summary

Table 10.7: Projected average changes in wave height, period and direction in Palau for December–March and June–September for RCP4.5 (low emissions, in blue) and RCP8.5 (very high emissions, in red), for two 20-year periods (2026–2045 and 2081–2100), relative to a 1986–2005 historical period. The values in brackets represent the 5th to 95th percentile range of uncertainty.

Variable	Season	2035	2090	Confidence (range)
Wave height change (m)	December–March	-0.0 (-0.3–0.3) -0.0 (-0.4–0.3)	-0.1 (-0.4–0.2) -0.2 (-0.4–0.1)	Low
	June–September	0.0 (-0.2–0.2) 0.0 (-0.2–0.2)	0.0 (-0.2–0.2) 0.0 (-0.2–0.2)	Low
Wave height change (ft)	December–March	-0.1 (-1.0–0.9) -0.1 (-1.2–1.0)	-0.3 (-1.3–0.7) -0.6 (-1.4–0.6)	Low
	June–September	0.0 (-0.5–0.8) -0.0 (-0.5–0.8)	0.0 (-0.5–0.7) 0.0 (-0.5–0.8)	Low
Wave period change (s)	December–March	-0.1(-0.4–0.3) -0.1 (-0.6–0.6)	-0.1 (-0.6–0.4) -0.2 (-0.8–0.4)	Low
	June–September	-0.0 (-0.6–0.5) -0.0 (-0.6–0.6)	-0.1 (-0.7–0.6) -0.1 (-0.8–0.5)	Low
Wave direction change (° clockwise)	December–March	0 (-5–5) 0 (-10–5)	-0 (-10–5) -5 (-10–5)	Low
	June–September	+0 (-30 tp 80) 0 (-0–60)	+0 (-30–80) +10 (-30–70)	Low

Wind-wave variables parameters are calculated for a 20-year period centred on 2035.